



**HAL**  
open science

# Rearrangement of the transmembrane domain interfaces associated with the activation 1 of a GPCR hetero-oligomer 2 3

Li Xue, Qian Sun, Han Zhao, Xavier Rovira, Siyu Gai, Qianwen He,  
Jean-Philippe Pin, Jianfeng Liu, Philippe Rondard

► **To cite this version:**

Li Xue, Qian Sun, Han Zhao, Xavier Rovira, Siyu Gai, et al.. Rearrangement of the transmembrane domain interfaces associated with the activation 1 of a GPCR hetero-oligomer 2 3. *Nature Communications*, 2019, 10 (1), pp.2765. 10.1038/s41467-019-10834-5. hal-02398123

**HAL Id: hal-02398123**

**<https://hal.science/hal-02398123>**

Submitted on 6 Dec 2019

**HAL** is a multi-disciplinary open access archive for the deposit and dissemination of scientific research documents, whether they are published or not. The documents may come from teaching and research institutions in France or abroad, or from public or private research centers.

L'archive ouverte pluridisciplinaire **HAL**, est destinée au dépôt et à la diffusion de documents scientifiques de niveau recherche, publiés ou non, émanant des établissements d'enseignement et de recherche français ou étrangers, des laboratoires publics ou privés.

1 **Rearrangement of the transmembrane domain interfaces associated with the activation**  
2 **of a GPCR hetero-oligomer**

3

4 Li Xue<sup>1</sup>, Qian Sun<sup>1</sup>, Han Zhao<sup>1</sup>, Xavier Rovira<sup>2,3</sup>, Siyu Gai<sup>1</sup>, Qianwen He<sup>1</sup>, Jean-Philippe  
5 Pin<sup>2</sup>, Jianfeng Liu<sup>1</sup> and Philippe Rondard<sup>2</sup>

6

7 <sup>1</sup> Cellular Signaling laboratory, International Research Center for Sensory Biology and  
8 Technology of MOST, Key Laboratory of Molecular Biophysics of MOE, and College of Life  
9 Science and Technology, Huazhong University of Science and Technology, Wuhan, Hubei  
10 430074, China

11 <sup>2</sup> Institut de Génomique Fonctionnelle (IGF), CNRS, INSERM, Université de Montpellier,  
12 Montpellier, France

13 <sup>3</sup> Present address : Molecular Photopharmacology Research Group, The Tissue Repair and  
14 Regeneration Laboratory, University of Vic - Central University of Catalonia, C. de la Laura,  
15 13, 08500 Vic, Spain.

16 These authors contributed equally : Li Xue, Qian Sun, Han Zhao, Xavier Rovira,

17

18

19 Correspondence and requests for materials should be addressed to J.-P.P (email : jean-  
20 philippe.pin@igf.cnrs.fr)

21 or to J.L. (email: jfliu@mail.hust.edu.cn)

22

23 **Abstract**

24

25 G protein-coupled receptors (GPCRs) can integrate extracellular signals via allosteric  
26 interactions within dimers and higher-order oligomers. However, the structural bases of these  
27 interactions remain unclear. Here, we use the GABA<sub>B</sub> receptor heterodimer as a model as it  
28 forms large complexes in the brain. It is subjected to genetic mutations mainly affecting  
29 transmembrane 6 (TM6) and involved in human diseases. By cross-linking, we identify the  
30 transmembrane interfaces involved in GABA<sub>B1</sub>-GABA<sub>B2</sub>, as well as GABA<sub>B1</sub>-GABA<sub>B1</sub>  
31 interactions. Our data are consistent with an oligomer made of a row of GABA<sub>B1</sub>. We bring  
32 evidence that agonist activation induces a concerted rearrangement of the various interfaces.  
33 While the GB1-GB2 interface is proposed to involve TM5 in the inactive state, cross-linking  
34 of TM6s lead to constitutive activity. These data bring insight for our understanding of the  
35 allosteric interaction between GPCRs within oligomers.

36

## 37 **Introduction**

38 G protein-coupled receptors (GPCRs) form the largest family of cell surface receptors  
39 and all cells are covered with dozens of different GPCR subtypes<sup>1</sup>. At the cellular level,  
40 multiple mechanisms have been identified that integrate the various GPCR-mediated signals.  
41 These mechanisms involve either cross-talk between signaling pathways<sup>2</sup>, or allosteric  
42 interactions between receptors associated in dimers or higher-order oligomers<sup>3-7</sup>. Although  
43 largely debated<sup>8,9</sup>, physical interactions between GPCRs allow either positive or negative  
44 cooperativity between protomers, both in homo-<sup>3,7,10,11</sup> and hetero-oligomers<sup>5,12-17</sup>. Recent  
45 studies highlight the potential role of such receptor assembly in physiopathological  
46 processes<sup>14,18-20</sup>.

47 Numerous structural, biophysical and biochemical studies have investigated the  
48 quaternary organization of GPCRs<sup>21-23</sup>. However, the structural bases for GPCR assembly and  
49 allosteric interaction remain elusive. To date, the most compelling studies revealed the  
50 transmembrane helices TM4 and TM5 on one hand, and TM1 and TM7 on the other hand,  
51 form possible dimerization interfaces<sup>20,24-27</sup>. Surprisingly, the amplitude of the conformational  
52 changes associated with ligand occupancy is limited at these proposed interfaces. This  
53 limitation makes a possible allosteric control of one subunit by the other difficult. This lack of  
54 a clear view of the interfaces involved in GPCR allosteric interactions may be due to the  
55 dynamic interaction between receptor molecules, as revealed by single-molecule studies<sup>24,28-</sup>  
56 <sup>30</sup>. Elucidating how oligomers assemble and how the subunits functionally interact is key for  
57 our understanding of their possible physiological significance.

58 The GPCR for  $\gamma$ -aminobutyric acid (GABA), the GABA<sub>B</sub> receptor, is involved in pre-  
59 and post-synaptic regulation of many synapses<sup>31</sup>. It is an excellent model to investigate the  
60 structural basis of cooperativity in higher-order oligomers for several reasons. i) The  
61 functional unit is a mandatory heterodimer of two homologous subunits GABA<sub>B1</sub> (GB1) and

62 GABA<sub>B2</sub> (GB2) (**Fig. 1a**)<sup>32</sup>. ii) Allosteric interactions between the seven transmembrane  
63 helices (7TMs) of GB1 and GB2 lead to improved coupling efficacy of GB2<sup>16</sup>. iii) GABA<sub>B</sub>  
64 receptors have the propensity to form stable hetero-oligomers organized through interactions  
65 between the GB1 subunits<sup>12,28,33-35</sup> (**Fig. 1b**). iv) Allosteric interactions between the  
66 heterodimeric units within such oligomers have been identified. These interactions allow a  
67 single heterodimer to bind ligand and activate G-proteins, within a tetrameric entity<sup>12,35</sup>.  
68 Despite this clear evidence of allosteric interactions between the subunits of the GABA<sub>B</sub>  
69 oligomer, and the known structure of the active and inactive heterodimeric extracellular  
70 domain<sup>36</sup>, little is known about 7TM structure.

71 Clarifying the structural bases of the allosteric interaction between GABA<sub>B</sub> subunits is  
72 critical, as this receptor is an interesting target for the treatment of various diseases, including  
73 spasticity, pain and alcoholism<sup>37</sup>. Moreover, recent studies revealed the GABA<sub>B</sub> receptor can  
74 be the target of auto-antibodies possibly at the origin of epilepsies and encephalitis<sup>38</sup>. In  
75 addition, mutations in the GABA<sub>B2</sub> receptor gene have been recently reported to be associated  
76 with Rett syndrome and epileptic encephalopathies<sup>39-41</sup>. Most of them correspond to residues  
77 in the TM6 helix that could point out outside of the 7TM core (**Fig. 1c**), while one was found  
78 in TM3 buried of the middle of the 7TM core<sup>40,41</sup>.

79 In this study, we reveal the 7TM domain interfaces in the GABA<sub>B</sub> oligomers and we  
80 also document their dynamics during receptor activation. Our data are consistent with a  
81 concerted reorientation of the subunits associated with receptor activation. Altogether, these  
82 data provide important information on how GABA<sub>B</sub> receptor oligomers are activated. Our  
83 data are more generally applicable to understanding the structural bases of the cooperativity  
84 observed in many GPCR dimers and higher-order oligomers.

## 85 **Results**

### 86 **GB1 and GB2 constructs for cross-linking experiments**

87 In this study, our aim was to identify the various interfaces involved in interaction of the  
88 GABA<sub>B</sub> receptor subunits in oligomers. For this, we decided to use cysteine cross-linking that  
89 gives a rather good resolution of the possible proximity between two residues in protein-  
90 protein interactions since it requires a distance below 8 Å between the Cβ of both cysteines.  
91 We was previously successfully used this approach to study the metabotropic glutamate  
92 receptor type 2 (mGlu2)<sup>42</sup>, that belong to the class C GPCRs as the GABA<sub>B</sub> receptor<sup>43</sup>. We  
93 used N-terminally SNAP-tagged GB1 and Halo-tagged GB2 (Fig. 2a) because they can be  
94 selectively and covalently labelled with non-cell permeant fluorescent substrates.  
95 Accordingly, only cell surface proteins are labelled, such that any oligomers retained in the  
96 intracellular compartment will not be detectable<sup>34,44</sup>. This is especially important in the case  
97 of the heterodimeric GABA<sub>B</sub> receptor for which one subunit (GB2) is required for the other  
98 (GB1) to reach the cell surface. Indeed, GB1 non associated with GB2 is retained in  
99 intracellular compartments<sup>45</sup>. With this approach both subunits can easily be detected by their  
100 fluorescence after SDS-PAGE in non-reducing conditions and protein-transfer to membranes,  
101 without the need of antibody labelling. SNAP-GB1 and Halo-GB2 have very similar  
102 molecular weights making distinguishing them difficult (**Fig. 2a**). Therefore, we shortened the  
103 C-terminal end of GB1 in our constructs and enlarged the C-terminal end of GB2 by adding a  
104 GFP tag. This gave easily distinguishable GB1 and GB2 subunits of 112 and 167 kDa  
105 respectively (Supplementary Figure 1a-b). Accordingly, the GB1-GB2 heterodimers (279  
106 kDa) can easily be separated from the GB1-GB1 dimer (224 kDa) by non-reducing SDS-  
107 PAGE (Supplementary Figure 1c). To prevent unwanted disulphide bridges, we mutated the  
108 cysteines of GB2 TM4 (Cys609<sup>4,45</sup> and Cys613<sup>4,49</sup>; see nomenclature of the class C GPCR  
109 7TMs<sup>46</sup>) to alanine (Supplementary Figure 2a). These constructs are named ‘control subunits’

110 and referred to GB1<sup>Ctr</sup> and GB2<sup>Ctr</sup> in this study (Fig. 2a). Finally, we verified that these two  
111 engineered subunits have similar cell surface targeting and functional properties to wild-types  
112 (Supplementary Figure 2b-c).

113

#### 114 **Characterization of the GB1-GB2 7TM dimer interface**

115 To characterize the GB1-GB2 interface, we examined inter-subunit cross-linking between  
116 GB1<sup>Ctr</sup> and GB2<sup>Ctr</sup> carrying one cysteine residue in all the TMs, except TM3 that is mainly  
117 buried into the 7TM domain (Fig. 2b-d; Supplementary Figure 3a-b, 4, 5 and 6). Only  
118 symmetric dimer interfaces were considered since the GABA<sub>B</sub> receptor ECD is symmetric<sup>36</sup>.  
119 Asymmetric interfaces have been less described in the GPCR family, and they are all  
120 computational studies<sup>24</sup>. Therefore, only GB1 and GB2 with a cysteine at the same position  
121 were co-expressed.

122 One needs to be cautious in interpreting the cross-linking results with membrane  
123 proteins from the blots analysis. A background for the dimer band is observed in most  
124 samples and is enhanced by the introduction of cysteines in many locations. It is probably due  
125 to non-specific cross-linking or non-specific association of the subunits upon denaturation.  
126 Non-specific cross-linking could occur at the cell surface spontaneously or during treatment  
127 with oxidative copper-phenanthrolin (CuP) before stopping the cross-linking reaction with the  
128 alkylating agent N-ethylmaleimide. Alternatively, Cys-crosslinking can occur after protein  
129 denaturation due to the exposure of buried Cys. Indeed, GB1<sup>Ctr</sup> and GB2<sup>Ctr</sup> retain some  
130 reactive cysteine residues that could form a spontaneous or CuP-induced disulphide bridge,  
131 though with low efficiency. In addition, non-specific association is expected to occur upon  
132 membrane protein denaturation, especially if the proteins are already associated in the plasma  
133 membrane, due to hydrophobic interactions between the unfolded protein chains. GB1<sup>Ctr</sup> and  
134 GB2<sup>Ctr</sup> retain the coiled-coil domain existing in the C-terminal region of the GABA<sub>B</sub> receptor

135 that can favour SDS-resistant dimers not necessarily covalently linked<sup>12,47</sup>, although they have  
136 not been observed by others<sup>48</sup>. In agreement, under basal conditions, a high variability in the  
137 ratio of GB1-GB2 dimer over the total of GB1 subunit is measured in the different  
138 experiments (Supplementary Figure 4). This probably results from differences in expression  
139 level and in sample preparation between the experiments. Of note, treatment with the reducing  
140 agent dithiothreitol (DTT) just before running the blots showed that a large part of the GB1-  
141 GB2 heterodimer band is resistant indicating that these dimers result from a non-specific  
142 protein association (Supplementary Figure 3b). Such band is most probably made of SDS-  
143 resistant heterodimers that are not covalently linked through a disulphide bridge between the  
144 GB1 and GB2 subunits.

145 Then to analyze specific Cys cross-linking, we concentrated our effort in identifying  
146 Cys positions for which a strong CuP induced cross-linking can be observed. CuP is used to  
147 promote Cys crosslinking<sup>42,49</sup> because spontaneous oxidation of the Cys residues located the  
148 plasma membrane is not efficient<sup>49,56</sup>. To determine the efficiency of cross-linking between  
149 the two subunits induced by CuP, we have quantified the change in the rate of GB1-GB2  
150 dimers to the total quantity of GB1 subunit detected on blots (Fig. 2d). The results revealed  
151 efficient cross-linking of GB1 and GB2 when Cys were introduced in TM5 or TM6. No such  
152 cross-linking was observed when Cys were introduced in TM1, 2, 4 or 7. No significant CuP-  
153 induced cross-linking was observed between GB1<sup>Ctr</sup> and GB2<sup>Ctr</sup> in which no Cys was  
154 introduced. These data strongly suggest that TM5 and TM6 of both subunits constitute the  
155 GB1-GB2 dimer interface (Fig. 2e).

156 Finally, we have to be aware of another possible limitation of our cysteine cross-  
157 linking strategy that is the trapping of interactions that can be transient, and some of them not  
158 being functionally relevant. It could be due to constant conformational dynamics of the  
159 proteins and their movement in the biological sample, or a cross-linking that could occur

160 during the sample preparation and experiments. In order to relate these interactions with  
161 functional properties of the receptor, we have performed these cross-linking experiments in  
162 presence of ligands known to stabilize the active or inactive conformations of the GABA<sub>B</sub>  
163 receptor.

164

### 165 **GB1-GB2 interface changes upon receptor activation**

166 We have then tested the dynamics of this interface. We have quantified the agonist effects on  
167 cross-linking to all the sites of the 7TM domains where Cys were introduced, including in  
168 TM5 and TM6 (Fig. 3a-c and Supplementary Figure 7a). In the presence of the agonist  
169 GABA, GB1-GB2 cross-linking between the two TM5s was largely decreased for two  
170 positions, indicating that the two TM5s are less close in the active state. However, inter-TM6  
171 cross-linking was strongly increased for several positions, indicated the two TM6s are become  
172 closer during activation. Based on these data, we propose a model where the GB1-GB2 dimer  
173 interface switches from TM5-6 in the absence of ligand (basal or inactive state) to mainly  
174 TM6 in the active conformation (Fig. 3d).

175 We were not surprised to observe GB1-GB1 cross-linking, when using a GB1 subunit  
176 carrying a Cys residue, as it was known that the GABA<sub>B</sub> receptor can associate into larger  
177 complexes likely through GB1-GB1 interaction<sup>12,35</sup> (Fig. 3a-b). However, consistent with our  
178 proposed model, there was a strong increase in GB1-GB1 dimers cross-linked through their  
179 TM5 upon agonist stimulation (Fig. 3a). In addition, the small amount of GB1-GB1 dimer  
180 cross-linked through their TM6 observed in the presence of the antagonist is no longer  
181 measured in the presence of the agonist (Fig. 3b). Of note, in these experiments the cross-  
182 linked bands were only partially decreased after DTT (Supplementary Figure 7b), suggesting  
183 that even after reduction of the cross-linked disulphide bridges, none covalent SDS resistant

184 interactions remain between GB1 and GB2, as discussed above, or between two GB1  
185 subunits<sup>50</sup>.

186 Overall, these data indicate a dynamic interaction between the subunits in the GABA<sub>B</sub>  
187 oligomer whereby GB1 TM6 switches from mainly contacting GB1 in the inactive state to  
188 contacting GB2 in the active state (Fig. 3d).

189

### 190 **Locking GB1-GB2 TM6 interface stabilizes an active state**

191 As our results suggest a TM6-TM6 interaction in the active state of the heterodimer, we  
192 postulated that this interface may be critical in the activation process since GB1 7TM strongly  
193 favours GB2 7TM coupling to G proteins<sup>16</sup>. We therefore cross-linked the TM6 domains in  
194 the heterodimer using the mutants GB1 I824C<sup>6.59</sup> and GB2 L711C<sup>6.59</sup> that had an efficient  
195 cross-linking between GB1 and GB2 at the TM6 level (Fig. 2d), but that could not be further  
196 increased by the agonist (Fig. 3c). Doing so, we observed a robust constitutive activity after  
197 CuP treatment in basal conditions (Fig. 4a). This constitutive activity was only slightly further  
198 stimulated by the full agonist GABA. This basal activity of the GABA<sub>B</sub> mutant correlated  
199 with the amount of receptor at the cell surface (Fig. 4b), and it cannot be blocked by the  
200 competitive antagonist (Fig. 4c). Importantly, CuP treatment itself had no effect on the  
201 GABA<sub>B</sub> receptor activity (Supplementary Figure 8a). In the absence of CuP treatment, these  
202 mutated GABA<sub>B</sub> constructs had a similar activity than the wild-type (Supplementary Figure  
203 8b-c). Conversely, when the putative inactive interface was stabilized by cross-linking  
204 GB1<sup>TM6</sup> with GB2<sup>TM4</sup> (Fig. 4d), using the mutants GB1 I824C<sup>6.59</sup> and GB2 A616C<sup>4.52</sup> that  
205 cross-linked well (Fig. 4e), the activation of the receptor by agonist was impaired (Fig. 4f).  
206 This activation is not completely suppressed likely because only a fraction of the receptors are  
207 cross-linked. Of note, the activation of the receptor by agonist was not impaired by the  
208 reversed pair GB1<sup>4.52</sup> with GB2<sup>6.59</sup>, and the GB1<sup>5.42</sup> with GB2<sup>5.42</sup> cross-linking

209 (Supplementary Figure 8d-e). It is probably because in these cross-linking experiments the  
210 oligomer is stabilized in a conformation closer to the active state by GB1-GB1 cross-linking  
211 through two GB1<sup>TM4</sup> and two GB1<sup>TM5</sup>, respectively (see below). Accordingly, the GB1-GB1  
212 dimer rate is strongly increased by the agonist in the GB1<sup>4.52</sup> with GB2<sup>6.59</sup> (Supplementary  
213 Figure 8e) and GB1<sup>5.42</sup> with GB2<sup>5.42</sup> (Fig. 3a).

214

### 215 **Model of the rearrangement at the 7TM heterodimer interface**

216 Based on the above experimental data, we propose a 3D model for the activation of the  
217 GABA<sub>B</sub> receptor, where in the inactive state, the heterodimer interface would be formed  
218 mainly by the two TM5s, plus GB1<sup>TM6</sup> and GB2<sup>TM4</sup> (Fig. 5a). During activation, a  
219 rearrangement of this interface would occur such that in the active state, the interface mainly  
220 involves the TM6s of both GB1 and GB2, as recently proposed in mGlu receptors<sup>42,51</sup>. Of  
221 note, our previous experimental data have shown a higher probability to cross-link TM4s in  
222 mGlu2 homodimers<sup>49</sup>, than in the GABA<sub>B</sub> heterodimer in this study. Indeed, we did not obtain  
223 any specific cross-linking between GB1-TM4 and GB2-TM4 in the resting (Supplementary  
224 Figure 3b) and active state of the receptor (Supplementary Figure 7a). We then propose that  
225 the amplitude of the relative reorientation between the 7TM dimer appears smaller in GB1-  
226 GB2 than in the mGlu2 homodimer (Fig. 5b). Our proposal is consistent with the observation  
227 of a smaller conformational change of the GABA<sub>B</sub> ECD compared to mGluR ECD, as  
228 previously reported based on crystal structures and FRET experiments<sup>36,52</sup>.

229

### 230 **GB1 7TM interaction in the oligomer during activation**

231 As observed above, GB1 mutants can be cross-linked not only with GB2 but also with  
232 themselves. It is consistent with the ability of GABA<sub>B</sub> receptors to form large complexes  
233 through GB1-GB1 interaction<sup>12,34</sup>. In order to identify the GB1 interfaces involved in the

234 formation of oligomers, we performed GB1-GB1 crosslinking in conditions where we would  
235 not have GB1-GB2 cross-linking. Therefore, we then examined the possible cross-linking  
236 between GB1<sup>Ctr</sup> subunits carrying one Cys residue in various TMs, co-expressed with GB2<sup>Ctr</sup>  
237 that do not contain introduced Cys (Fig. 6a-b).

238 Under basal conditions, CuP treatment resulted in a strong increase of GB1-GB1  
239 cross-linked dimers for the cysteine mutant in TM4 and TM6 (Fig. 6c), where a single Cys  
240 mutation was introduced either in GB1<sup>TM4</sup> or in GB1<sup>TM6</sup>. In the same conditions, CuP  
241 treatment increased GB1-GB1 cross-linked dimers to a lower extent for TM1, TM5 and TM7  
242 (Fig. 6d). These results suggest there are higher-order oligomers in the inactive state, where  
243 one GB1 subunit forms two different interfaces with two other GB1s, one mediated by TM4  
244 and the other by TM6 (Fig. 6e). This model is also consistent with the GB1<sup>TM5</sup>-GB2<sup>TM5</sup>  
245 interface we proposed for the GABA<sub>B</sub> heterodimer in the inactive state, where both TM5s are  
246 buried in the interface of the heterodimer (Fig. 5a), then the probability of two GB1<sup>TM5</sup> being  
247 crosslinked in the inactive state is low.

248 In contrast, a strong increase of the GB1-GB1 cross-linking was induced by agonist  
249 for Cys located in TM1, TM5 and TM7 (Fig. 6d), but to a lower extent for TM4 while no  
250 significant change was obtained for TM6 (Fig. 6c). These results indicate that two main  
251 interfaces are formed between the GB1 subunits in the higher-order oligomers during  
252 activation, one being TM5 and the other TM1-TM7 interface (Fig. 6f). This active state of the  
253 oligomers is consistent with the movement of GB1<sup>TM6</sup> that switches to the GB2 interface  
254 during activation (Fig. 5a). Such reorientation of GB1<sup>TM6</sup> should limit its exposure to form  
255 cross-linking with another GB1<sup>TM6</sup>, consistent with no increase in cross-linking between two  
256 GB1<sup>TM6</sup> upon agonist treatment (Fig. 6c). Of note, in these experiments the GB1-GB1 cross-  
257 linked bands were only partly sensitive to DTT (Supplementary Figure 9), suggesting that

258 even after reduction of the cross-linked disulphide bridges, none covalent but strong  
259 interactions remain between GB1 subunits, as stated above.

260

### 261 **Model of the two interfaces between GB1s in oligomers**

262 To further support this oligomerization model and validate which GB1-GB1 interfaces are  
263 made at a given time, we measured the high-molecular weight species formed by the cross-  
264 linked GB1 subunits. We explored which pairs of cysteines introduced in the GB1 7TM cause  
265 higher-order oligomers, when co-expressed with a non-mutated GB2 (Fig. 7a; Supplementary  
266 Figure 10a). These high-molecular-weight complexes only formed for those mutants of GB1  
267 that can form one interface through two GB1<sup>TM4</sup> or GB1<sup>TM5</sup> and another interface between  
268 two GB1<sup>TM1</sup>, GB1<sup>TM6</sup> or GB1<sup>TM7</sup> (Fig. 7b). There were no high-molecular-weight complexes  
269 with GB1<sup>Ctr</sup> co-expressed with GB2<sup>Ctr</sup>, and also with most of GB1 double mutants co-  
270 expressed with GB2<sup>Ctr</sup> (Fig. 7a; Supplementary Figure 10a). These oligomers are consistent  
271 with the cross-linking of at least three GB1 subunits through two different interfaces of GB1  
272 in the inactive state, one mediated by TM4s or/and TM5s and the other by TM1s, TM6s or  
273 TM7s (Fig. 7c). Of note, in these experiments the oligomer cross-linked bands were sensitive  
274 to DTT (Supplementary Figure 10b) although that not totally, suggesting none covalent but  
275 strong interactions remain between GB1 subunits, as stated above.

276 Interestingly, receptor activation increased the intensity of the oligomeric band when  
277 the symmetric GB1<sup>TM4</sup> interface was cross-linked together with GB1<sup>TM1</sup> or GB1<sup>TM7</sup> interface  
278 (Fig. 7a). In addition, the symmetric GB1<sup>TM5</sup> interface was cross-linked together with  
279 GB1<sup>TM1</sup>. These results are consistent with the active state of the oligomers proposed above  
280 (Fig. 6f). Of note, our data suggested that a simultaneous cross-linking of the two interfaces  
281 mediated by TM5s and TM7s within the same GB1 subunit to form oligomers is not possible.  
282 Indeed, a double mutant of GB1 carrying one cysteine in TM5 (I771C<sup>5,42</sup>) and one in TM7

283 (L838C<sup>7,34</sup>) produced no oligomer but the GB1-GB1 dimer rate that was further increased by  
284 GABA (Fig. 7a). In contrast the simultaneous GB1 two interfaces TM5s/TM1s, TM4s/TM1s  
285 or TM4s/TM7s are possible.

286

### 287 **A disease-causing mutation stabilizes the active interfaces**

288 We have introduced the genetic mutation S694I<sup>6,42</sup> in our rat GB2 constructs (equivalent to  
289 genetic mutation S695I<sup>6,42</sup> in human GB2), that produced a strong constitutive activity of the  
290 the GABA<sub>B</sub> receptor (Supplementary Fig. 11), and as recently reported<sup>47</sup>. In the absence of  
291 agonist, this mutation stabilized the active interface of the heterodimer unit mediated by both  
292 TM6s as measured by the increased GB1-GB2 cross-linked upon CuP treatment (Fig. 8a-b).  
293 In addition, this mutation stabilized the active interface between the GB1 subunits in the  
294 oligomer in the basal state, as measured by a strong crosslinking between the GB1 TM5s  
295 upon CuP treatment (Fig. 8c-d). Altogether these data are consistent with a constitutive  
296 activity of the receptor induced by this mutation. This later is also associated with the  
297 stabilization of an oligomer organized in an active assembly.

298

### 299 **Model of the active and inactive 7TM oligomer interfaces**

300 Altogether, on the basis of the cysteine cross-linking results, we propose a 3D model of the  
301 7TM oligomer using four molecules of heterodimers, named *A-D* (Fig. 9). In the resting state,  
302 one heterodimer interacts with two others through the GB1 subunits, through two symmetric  
303 interfaces mediated by GB1<sup>TM4</sup> and GB1<sup>TM6</sup> that are on the opposite face of GB1 (Fig. 9a).  
304 Accordingly, GB1<sup>TM4</sup> of the heterodimer *B* interacts with GB1<sup>TM4</sup> of the heterodimer *C*, while  
305 GB1<sup>TM6</sup> of the heterodimer *B* interacts with the GB1<sup>TM6</sup> of the heterodimer *A*. In the active  
306 state, two new interfaces are formed: (i) a GB1 interface TM4-TM5 made by the heterodimers

307 *B* and *C*; (ii) a GB1 interface TM1-TM7 between the heterodimers *A* and *B* (Fig. 9b). Our  
308 model is compatible with the reorientation of the TM5s and TM6s at the interface between  
309 GB1 and GB2 during activation, as proposed above (Fig. 5a). Finally, this active state of the  
310 oligomer allows the coupling of one G-protein by dimer (Fig. 9c).

311 **Discussion**

312 The GABA<sub>B</sub> receptor was the first clear example of a mandatory heterodimeric  
313 GPCR<sup>53</sup>, and this discovery stimulated research on the putative dimerization of other GPCRs.  
314 Furthermore, the GABA<sub>B</sub> receptor was more recently shown to associate into larger  
315 complexes made of two or more heterodimers<sup>12,28,34</sup>, and this was confirmed in native tissues  
316 in several ways<sup>12,54,55</sup>. However, the structural bases of the interactions are still unclear. Here,  
317 using Cys cross-linking experiments, we propose a model for the GABA<sub>B</sub> 7TM assembly  
318 within a GABA<sub>B</sub> oligomer, involving dynamic and concerted movements between the  
319 subunits associated with receptor activation. Interestingly, we identified TM6, the TM known  
320 to undergo major conformational change upon GPCR activation<sup>56,57</sup>, to switch interfaces.  
321 Furthermore, we demonstrate that a TM6-TM6 interaction between GB1 and GB2 is  
322 sufficient for receptor activation.

323 We propose an organization of the GABA<sub>B</sub> higher-order oligomers in rows at the  
324 surface of live cells. Within these oligomers, GB1 subunits are assembled in lines via two  
325 opposite sides of their 7TMs, while the GB2 subunits are on the side. This model is supported  
326 by the large FRET signal previous reported between GB1 subunits, and a quasi-absence of  
327 FRET between GB2 N termini<sup>12,34</sup>, even though GB2 subunits co-diffuse at the neuronal  
328 surface indicating they are in the same receptor complex<sup>54</sup>. This organization may also  
329 explain the observed ordered arrays of GABA<sub>B</sub> receptors in transfected cells<sup>28</sup>. In class A  
330 GPCRs, similar rows have also been proposed for the organization of rhodopsin<sup>21,22</sup>, a  
331 structure that could be destabilized by genetic mutations at the TM1 and TM5 interfaces then  
332 leading to retinitis pigmentosa<sup>20</sup>. Our data suggest that rows of GABA<sub>B</sub> receptors may form  
333 spontaneously through two distinct GB1 interfaces, TM4-5 and TM1-7. This GABA<sub>B</sub> receptor  
334 organization is consistent with the proposed interfaces involved in many class A GPCR  
335 oligomerization<sup>23,49,58</sup>, for which both TM4-5 and TM1-7 were the most frequently

336 proposed<sup>24,26</sup>.

337 In the GABA<sub>B</sub> oligomers, we propose that a dimer of dimers can form a minimal  
338 repeat unit. This tetramer is stabilized by interactions between the two GB1 subunits through  
339 their symmetric TM1-TM7 interface in the active state (Fig. 9b). This model is supported by  
340 the organization of the GABA<sub>B</sub> ECD in a tetramer, stabilized by interactions between the  
341 lobes 2 (lower lobes) of two GB1 VFTs<sup>12</sup>. As a consequence of this tetramer organization, the  
342 higher-order oligomers would be stabilized by the symmetric GB1<sup>TM4</sup> interface between two  
343 tetramers. Interestingly, when active G-protein is added to the receptor in our 3D model, the  
344 G-protein interacts with two GB1 subunits within the same tetramer. Most important, it is  
345 even possible for two G-proteins to couple to one GABA<sub>B</sub> tetramer (Fig. 9c). Thus the  
346 hypothesis that only one G-protein is activated by a tetramer<sup>12</sup> could not be explained by  
347 structural steric reasons at the level of the 7TMs. Instead, it could be due to the negative  
348 allosteric between two heterodimers within a tetramer, as recently reported for the GABA<sub>B</sub>  
349 ECDs<sup>35</sup>.

350 In our model, the GABA<sub>B</sub> tetramer has a rhomboid shape structure. Rhomboids that  
351 has been proposed for several class A GPCRs that form spontaneous tetramers<sup>23,58</sup>. In  
352 addition, a rhomboid organization for the tetramer could explain the smaller amplitude of the  
353 relative reorientation in GABA<sub>B</sub> 7TM heterodimer compared to the 7TM of mGlu2 dimers  
354 that do not form constitutive oligomers<sup>34,59,60</sup>. This small rearrangement between the two  
355 7TMs in the GABA<sub>B</sub> receptor heterodimer is also consistent with the limited conformational  
356 changes between the active and inactive states at the level of the ECDs<sup>36</sup>, and the negative  
357 allosteric between the two heterodimers<sup>35</sup>.

358 We demonstrate here that the GB1-GB2 heterodimer is the minimal functional unit  
359 within tetramers. This is best illustrated by the receptor full constitutive activity resulting  
360 from GB1<sup>TM6</sup>-GB2<sup>TM6</sup> crosslinking. A key determinant of a tetramer is the TM6 of GB1, that

361 binds another GB1, in the inactive state, but binds GB2 in the active state. This concerted  
362 rearrangement of the various interfaces of GB1 during activation could be responsible for the  
363 positive cooperativity between the two 7TMs in the heterodimer. Indeed, we have previously  
364 demonstrated that the GB1 7TM activation is critical for stabilizing the active state for GB2  
365 activation<sup>16</sup>.

366 The switching of GB1<sup>TM6</sup> from one interface to another during activation could be also  
367 responsible for the asymmetric activation of the two 7TMs in the heterodimer. Indeed, both  
368 GB1<sup>TM6</sup> and the G-protein could be responsible for allowing a single 7TM domain in a  
369 heterodimer to reach a conformation compatible with G-protein activation<sup>32</sup>. Similarly in the  
370 homodimeric and heterodimeric mGluRs, one TM6 in the dimer could also be responsible for  
371 the asymmetric functioning of the 7TMs, where only one subunit of the dimer couples to the  
372 G-protein<sup>15</sup>. Indeed, in the mGlu2-4 and GABA<sub>B</sub> heterodimers, the G-protein is only activated  
373 by one of the subunits, namely mGlu4 and GB2, respectively. In these heterodimers,  
374 functional asymmetry is not due to the fact that it is only the G-protein-bound subunit that can  
375 change its conformation. Indeed, the associated subunit also reaches a specific conformation  
376 that positively acts on the G-protein-activating subunit<sup>15,16</sup>. The asymmetric functioning of  
377 TM6, as indicated by our data on GABA<sub>B</sub> and mGlu receptors, likely explains the allosteric  
378 interaction within class A GPCR dimers. Indeed, in many cases, a negative allosteric  
379 interaction has been reported, with one subunit only being able to reach a G-protein activating  
380 state<sup>3,61</sup>.

381 The dynamic changes we observe at TM6 help to explain the many disease mutations  
382 there<sup>39-41</sup>. Interestingly, several of these mutations in GB2<sup>TM6</sup> including those localized near  
383 the extracellular part of TM6 produce a GABA<sub>B</sub> receptor that is constitutively active,  
384 suggesting the mutations favor GB1<sup>TM6</sup>-GB2<sup>TM6</sup> interactions, as demonstrated by one of them  
385 in the present study. Finally, auto-antibodies against the GB1 ECD were identified in a

386 number of patients with encephalitis leading to loss of function of GABA<sub>B</sub> receptor<sup>38,62</sup>. The  
387 large and concerted movement proposed during activation of the GABA<sub>B</sub> oligomer offers  
388 multiple inroads for these antibodies to affect GABA<sub>B</sub> function.

389         In summary, we provide a model of dynamic interaction between 7TM protein  
390 subunits in a well-recognized oligomer, and we propose a key role for TM6 in this process.  
391 Although our model starts to explain allosteric interaction between GPCRs, these findings  
392 may be specific for the GABA<sub>B</sub> receptor, and other class C GPCRs or all GPCRs. These data  
393 provide the steps and future studies will determine the general applicability of the structural  
394 organization and allostery to GPCR dynamics.

395

396

397 **Methods**

398 **Materials**

399 GABA ( $\gamma$ -aminobutyric acid) and dichloro(1,10-phenanthroline)copper(II) were purchased  
400 from Sigma-Aldrich (St. Louis, MO, USA). CGP54626 was from Tocris Bioscience  
401 (Ellisville, MO, USA). Lipofectamine 2000 and Fluo4-AM were obtained from Life  
402 Technologies (Carlsbad, CA, USA). SNAP-Surface<sup>®</sup> Alexa Fluor<sup>®</sup> 647 was from New  
403 England Biolabs, whereas HaloTag<sup>®</sup> Alexa Fluor<sup>®</sup> 660 was from Promega (Beijing) Biotech  
404 Co., Ltd.

405

406 **Plasmids and transfection**

407 The pRK5 plasmids encodes either the wild-type rat GB1a, tagged with HA and SNAP  
408 inserted just after the signal or the wild-type rat GB2 tagged with Flag and Halo inserted just  
409 after the signal peptide (Supplementary Figure 12). GB1<sup>Ctr</sup> was obtained from rat GB1a wild-  
410 type sequence by deleting the last 32 amino acids encoding for GB1. GB2<sup>Ctr</sup> was obtained  
411 from rat GB2 wild-type sequence by adding a GFP-tag at the C-terminal end of GB2. The  
412 cysteine substitutions were generated by site-directed mutagenesis using the QuikChange  
413 mutagenesis protocol (Agilent Technologies) using the primers described in Supplementary  
414 Figure 13 and Supplementary Figure 14 for the GB1 and GB2 mutants, respectively.

415 HEK293 cells (ATCC, CRL-1573) were cultured in Dulbecco's modified Eagle's medium  
416 (DMEM) supplemented with 10% FBS and transfected by electroporation. Unless stated  
417 otherwise,  $10^7$  cells were transfected with plasmid DNA containing the coding sequence of  
418 the receptor subunits, and completed to a total amount of 10  $\mu$ g of plasmid DNA with the  
419 empty vector pRK5. For the determination of intracellular calcium measurements and inositol  
420 phosphate (IP) accumulation, the cells were also transfected with the chimeric G-protein Gq<sub>i9</sub>,  
421 which allows the coupling of the recombinant GABA<sub>B</sub> receptor to the phospholipase C<sup>52</sup>.

422

423

#### 424 **Cross-linking and fluorescent-labeled blot experiments**

425 48 h after electroporation, adherent HEK293 cells plated in 12-well plates were labeled with  
426 100 nM SNAP-Green and 3.5  $\mu$ M Halo-Red in culture medium at 37°C for 1 h. Then, cells  
427 were incubated with drug (each at 100  $\mu$ M) or PBS at 37°C for 30 min. Afterwards, cross-link  
428 buffer (1.5 mM Cu(II)-(o-phenanthroline), 1 mM CaCl<sub>2</sub>, 5 mM Mg<sup>2+</sup>, 16.7 mM Tris, pH 8.0,  
429 100 mM NaCl) was added at room temperature for 20 min. After incubation with 10 mM N-  
430 ethylmaleimide at 4°C for 15 min to stop the cross-linking reaction, cells were lysed with  
431 lysis buffer (containing 50 mM Tris (pH 7.4), 150 mM NaCl, 1% NP-40, 0.5% sodium  
432 deoxycholate) at 4°C for 1h. After centrifugation at 12 000 g for 30 min at 4°C, supernatants  
433 were mixed with loading buffer at 37°C for 10 min. In reducing conditions, samples were  
434 treated with 100 mM DTT in loading buffer for 10 min before loading the samples. Equal  
435 amounts of proteins were resolved by 29:1 acrylamide:bisacrylamide and 3-9 % SDS-PAGE.  
436 For oligomer analysis, 59:1 acrylamide:bisacrylamide and 6 % SDS-PAGE were used.  
437 Proteins were transferred to nitrocellulose membranes (Millipore). Membrane were imaged on  
438 an Odyssey CLx imager (LI-COR Bioscience, Lincoln, NE, USA) at 600 nm and 700 nm.

439

#### 440 **Cell surface quantification**

441 Detection of the HA- and Flag-tagged constructs at the cell surface by ELISA was performed.  
442 24 h after transfection, the HEK293 cells were fixed with 4% paraformaldehyde, blocked with  
443 10% FBS. HA-tagged constructs were detected with a monoclonal rat anti-HA antibody 3F10  
444 (Roche) at 0.5  $\mu$ g/mL and goat anti-rat antibodies coupled to horseradish peroxidase  
445 (Jackson Immunoresearch, West Grove, PA) at 1.0  $\mu$ g/mL. Flag-tagged constructs  
446 were detected with the mouse monoclonal anti-Flag antibody M2 (Sigma, St. Louis,

447 MO) at 0.8 µg/mL and goat anti-mouse antibodies coupled to horseradish peroxidase  
448 (Amersham Biosciences, Uppsala, Sweden) at 0.25 µg/mL. Bound antibodies coupled to  
449 horseradish peroxidase were detected by chemoluminescence using SuperSignal substrate  
450 (Pierce) and a 2103 EnVision™ Multilabel Plate Reader (Perkin Elmer, Waltham, MA,  
451 USA).

452 The amounts of SNAP-tagged constructs at the cell surface were quantified by fluorescence.  
453 Briefly, HEK293 cells expressing SNAP-tagged constructs were incubated at 37°C for 1 h  
454 with 300 nM of the SNAP-Lumi4-Tb substrate, then washed three times with Tag-Lite buffer.  
455 After excitation with a laser at 337 nm, the fluorescence of the Lumi4-Tb was collected at 620  
456 nm for 450 µs after a 50-µs delay on a PHERAstar FS (BMG Labtech, Ortenberg, Germany)  
457 <sup>63</sup>.

458

#### 459 **Inositol phosphate measurements**

460 Inositol phosphate accumulation in HEK293 cells was measured using the IP-One HTRF kit  
461 (Cisbio Bioassays) according to the manufacturer's recommendations.

462

#### 463 **Intracellular calcium release measurements**

464 Twenty-four hours after transfection with plasmids encoding the indicated GABA<sub>B</sub> subunits  
465 and a chimeric protein Gqi9, HEK-293 cells were washed with HBSS buffer (20 mM Hepes,  
466 1 mM MgSO<sub>4</sub>, 3.3 mM Na<sub>2</sub>CO<sub>3</sub>, 1.3 mM CaCl<sub>2</sub>, 0,1% BSA, 2.5 mM probenecid) and loaded  
467 with 1 µM Ca<sup>2+</sup>-sensitive fluorescent dye Fluo-4 AM (Molecular Probes, Eugene, OR, USA)  
468 for 1 h at 37°C. After a wash, cells were incubated with 50 µl of buffer and 50 µl of 2X-  
469 GABA solution at various concentrations was added after 20 s of recording. Fluorescence  
470 signals (excitation 485 nm, emission 525 nm) were measured by using the fluorescence  
471 microplate reader Flexstation (Molecular Devices, Sunnyvale, CA, USA) at sampling

472 intervals of 1.5 s for 60 s. Data were analyzed with the program Soft Max Pro (Molecular  
473 Devices, Sunnyvale, CA, USA). Dose-response curves were fitted using Prism (GraphPad  
474 software, San Diego, CA, USA).

475

#### 476 **Molecular modeling**

477 The molecular model of GB1 and GB2 7TM were generated with Modeller 9.18<sup>64</sup> based on  
478 the crystal structure of the mGluR1 receptor (PDB code 4OR2<sup>65</sup>) using the loop optimization  
479 method. The sequence of all GABA<sub>B</sub> and mGlu subtypes for rat and human species were  
480 aligned with ClustalW2<sup>66</sup>. Then, the sequences of mGluR1, GB1 and GB2 were extracted and  
481 used to build the model. From 100 models generated, the top ten classified by DOPE score  
482 were visually inspected, and the best scored structure with suitable loops was chosen<sup>67</sup>.

483 The active and inactive dimeric arrangement of the GABA<sub>B</sub> 7TMs was built by superposition  
484 to the different dimer structures of the previously reported mGlu<sub>2</sub> model<sup>42</sup> until the position of  
485 GB1 and GB2 was compatible with the enhanced cross-linking found in presence of the  
486 agonist molecule. The intermediate states were generated from the mGluR2 7TM intermediate  
487 models, which are in accordance with the dynamic transition expected from the inactive to the  
488 active state. The tetrameric and oligomeric forms in active and inactive states were built by  
489 translating and rotating active and inactive GABA<sub>B</sub> dimers with PyMOL software (Palo Alto,  
490 CA, USA) in a position compatible with the enhanced cross-linking between two GABA<sub>B1</sub>  
491 protomers found in resting state and in presence of the agonist molecule. The oligomeric  
492 active state of a GABA<sub>B</sub> 7TM in complex with the G-protein was built using as a template the  
493 crystal structure of the active  $\beta_2$  adrenergic receptor (PDB code 3SN6<sup>68</sup>). The sequence  
494 alignment was based on the structural superposition of the  $\beta_2$  adrenergic receptor and GB2.  
495 To build the model of the active dimeric arrangement of GABA<sub>B</sub> in complex with the G-

496 protein, the G-protein atomic coordinates (PDB code 3SN6) were transferred to the active  
497 GB2 7TM subunit.

498 Images based on the different states modeled from inactive to active, were calculated using  
499 UCSF Chimera software<sup>69</sup>. Discovery studio visualizer (Accelrys Software Inc., San Diego,  
500 CA, USA) was used for protein structure visualization and PDB file editing purposes.  
501 Multiple sequence alignment visualization and analysis were performed with Jalview  
502 software<sup>70</sup>.

503

#### 504 **Curve fitting and data analysis**

505 Curve fitting was performed using nonlinear regression using GraphPad Prism 7 software. P-  
506 values were determining using a paired or unpaired t test with Welch's correction.

507

#### 508 **Data Availability**

509 Data supporting the findings of this manuscript are available from the corresponding authors  
510 upon reasonable request. A reporting summary for this Article is available as a  
511 Supplementary Information file.

512

513 The source data underlying Figs. 2c-d, 3a-b, 4a-c, 4e-f, 6c-d, 7a, 8a, 8c and Supplementary  
514 Figs 8a, 8d, 10a, 11 are provided as a Source Data file.

515

516

517

518

519

520

521

522

523

524

525

526

528

- 529 1. Hauser, A.S., Attwood, M.M., Rask-Andersen, M., Schioth, H.B. & Gloriam, D.E.  
530 Trends in GPCR drug discovery: new agents, targets and indications. *Nat Rev Drug*  
531 *Discov* **16**, 829-842 (2017).
- 532 2. Prezeau, L. et al. Functional crosstalk between GPCRs: with or without  
533 oligomerization. *Curr Opin Pharmacol* **10**, 6-13 (2010).
- 534 3. Albizu, L. et al. Time-resolved FRET between GPCR ligands reveals oligomers in  
535 native tissues. *Nat Chem Biol* **6**, 587-594 (2010).
- 536 4. Cordeaux, Y. & Hill, S.J. Mechanisms of cross-talk between G-protein-coupled  
537 receptors. *Neurosignals* **11**, 45-57 (2002).
- 538 5. Damian, M. et al. GHSR-D2R heteromerization modulates dopamine signaling  
539 through an effect on G protein conformation. *Proc Natl Acad Sci U S A* **115**, 4501-  
540 4506 (2018).
- 541 6. Ferre, S. et al. G protein-coupled receptor oligomerization revisited: functional and  
542 pharmacological perspectives. *Pharmacol Rev* **66**, 413-434 (2014).
- 543 7. Smith, N.J. & Milligan, G. Allostery at G protein-coupled receptor homo- and  
544 heteromers: uncharted pharmacological landscapes. *Pharmacol Rev* **62**, 701-725  
545 (2010).
- 546 8. Bouvier, M. & Hebert, T.E. CrossTalk proposal: Weighing the evidence for Class A  
547 GPCR dimers, the evidence favours dimers. *J Physiol* **592**, 2439-2441 (2014).
- 548 9. Lambert, N.A. & Javitch, J.A. CrossTalk opposing view: Weighing the evidence for  
549 class A GPCR dimers, the jury is still out. *J Physiol* **592**, 2443-2445 (2014).
- 550 10. Birdsall, N.J. Class A GPCR heterodimers: evidence from binding studies. *Trends*  
551 *Pharmacol Sci* **31**, 499-508 (2010).
- 552 11. Springael, J.Y., Urizar, E., Costagliola, S., Vassart, G. & Parmentier, M. Allosteric  
553 properties of G protein-coupled receptor oligomers. *Pharmacol Ther* **115**, 410-418  
554 (2007).
- 555 12. Comps-Agrar, L. et al. The oligomeric state sets GABA(B) receptor signalling  
556 efficacy. *EMBO J* **30**, 2336-2349 (2011).
- 557 13. Gomes, I. et al. G Protein-Coupled Receptor Heteromers. *Annu Rev Pharmacol*  
558 *Toxicol* **56**, 403-425 (2016).
- 559 14. Gonzalez-Maeso, J. et al. Identification of a serotonin/glutamate receptor complex  
560 implicated in psychosis. *Nature* **452**, 93-97 (2008).
- 561 15. Liu, J. et al. Allosteric control of an asymmetric transduction in a G protein-coupled  
562 receptor heterodimer. *Elife* **6** (2017).
- 563 16. Monnier, C. et al. Trans-activation between 7TM domains: implication in  
564 heterodimeric GABAB receptor activation. *EMBO J* **30**, 32-42 (2011).
- 565 17. Moreno Delgado, D. et al. Pharmacological evidence for a metabotropic glutamate  
566 receptor heterodimer in neuronal cells. *Elife* **6** (2017).
- 567 18. Bonaventura, J. et al. Allosteric interactions between agonists and antagonists within  
568 the adenosine A2A receptor-dopamine D2 receptor heterotetramer. *Proc Natl Acad Sci*  
569 *U S A* **112**, E3609-3618 (2015).
- 570 19. Kern, A., Albarran-Zeckler, R., Walsh, H.E. & Smith, R.G. Apo-ghrelin receptor  
571 forms heteromers with DRD2 in hypothalamic neurons and is essential for  
572 anorexigenic effects of DRD2 agonism. *Neuron* **73**, 317-332 (2012).
- 573 20. Ploier, B. et al. Dimerization deficiency of enigmatic retinitis pigmentosa-linked  
574 rhodopsin mutants. *Nat Commun* **7**, 12832 (2016).

- 575 21. Fotiadis, D. et al. Atomic-force microscopy: Rhodopsin dimers in native disc  
576 membranes. *Nature* **421**, 127-128 (2003).
- 577 22. Gunkel, M. et al. Higher-order architecture of rhodopsin in intact photoreceptors and  
578 its implication for phototransduction kinetics. *Structure* **23**, 628-638 (2015).
- 579 23. Marsango, S., Ward, R.J., Alvarez-Curto, E. & Milligan, G. Muscarinic receptor  
580 oligomerization. *Neuropharmacology* **136**, 401-410 (2018).
- 581 24. Dijkman, P.M. et al. Dynamic tuneable G protein-coupled receptor monomer-dimer  
582 populations. *Nat Commun* **9**, 1710 (2018).
- 583 25. Manglik, A. et al. Crystal structure of the micro-opioid receptor bound to a morphinan  
584 antagonist. *Nature* **485**, 321-326 (2012).
- 585 26. Mondal, S. et al. Membrane driven spatial organization of GPCRs. *Sci Rep* **3**, 2909  
586 (2013).
- 587 27. Tanaka, T., Nomura, W., Narumi, T., Masuda, A. & Tamamura, H. Bivalent ligands of  
588 CXCR4 with rigid linkers for elucidation of the dimerization state in cells. *J Am Chem*  
589 *Soc* **132**, 15899-15901 (2010).
- 590 28. Calebiro, D. et al. Single-molecule analysis of fluorescently labeled G-protein-coupled  
591 receptors reveals complexes with distinct dynamics and organization. *Proc Natl Acad*  
592 *Sci U S A* **110**, 743-748 (2013).
- 593 29. Hern, J.A. et al. Formation and dissociation of M1 muscarinic receptor dimers seen by  
594 total internal reflection fluorescence imaging of single molecules. *Proc Natl Acad Sci*  
595 *U S A* **107**, 2693-2698 (2010).
- 596 30. Kasai, R.S. & Kusumi, A. Single-molecule imaging revealed dynamic GPCR  
597 dimerization. *Curr Opin Cell Biol* **27**, 78-86 (2014).
- 598 31. Gassmann, M. & Bettler, B. Regulation of neuronal GABA(B) receptor functions by  
599 subunit composition. *Nat Rev Neurosci* **13**, 380-394 (2012).
- 600 32. Pin, J.P. & Bettler, B. Organization and functions of mGlu and GABAB receptor  
601 complexes. *Nature* **540**, 60-68 (2016).
- 602 33. Comps-Agrar, L., Kniazeff, J., Brock, C., Trinquet, E. & Pin, J.P. Stability of GABAB  
603 receptor oligomers revealed by dual TR-FRET and drug-induced cell surface  
604 targeting. *FASEB J* **26**, 3430-3439 (2012).
- 605 34. Maurel, D. et al. Cell-surface protein-protein interaction analysis with time-resolved  
606 FRET and snap-tag technologies: application to GPCR oligomerization. *Nat Methods*  
607 **5**, 561-567 (2008).
- 608 35. Stewart, G.D., Comps-Agrar, L., Norskov-Lauritsen, L.B., Pin, J.P. & Kniazeff, J.  
609 Allosteric interactions between GABAB1 subunits control orthosteric binding sites  
610 occupancy within GABAB oligomers. *Neuropharmacology* **136**, 92-101 (2018).
- 611 36. Geng, Y., Bush, M., Mosyak, L., Wang, F. & Fan, Q.R. Structural mechanism of  
612 ligand activation in human GABA(B) receptor. *Nature* **504**, 254-259 (2013).
- 613 37. Bowery, N.G. GABAB receptor: a site of therapeutic benefit. *Curr Opin Pharmacol* **6**,  
614 37-43 (2006).
- 615 38. Dalmau, J. & Graus, F. Antibody-Mediated Encephalitis. *N Engl J Med* **378**, 840-851  
616 (2018).
- 617 39. Hamdan, F.F. et al. High Rate of Recurrent De Novo Mutations in Developmental and  
618 Epileptic Encephalopathies. *Am J Hum Genet* **101**, 664-685 (2017).
- 619 40. Vuillaume, M.L. et al. A novel mutation in the transmembrane 6 domain of GABBR2  
620 leads to a Rett-like phenotype. *Ann Neurol* **83**, 437-439 (2018).
- 621 41. Yoo, Y. et al. GABBR2 mutations determine phenotype in rett syndrome and epileptic  
622 encephalopathy. *Ann Neurol* **82**, 466-478 (2017).
- 623 42. Xue, L. et al. Major ligand-induced rearrangement of the heptahelical domain  
624 interface in a GPCR dimer. *Nat Chem Biol* **11**, 134-140 (2015).

- 625 43. Kniazeff, J., Prezeau, L., Rondard, P., Pin, J.P. & Goudet, C. Dimers and beyond: The  
626 functional puzzles of class C GPCRs. *Pharmacol Ther* **130**, 9-25 (2011).
- 627 44. Scholler, P. et al. HTS-compatible FRET-based conformational sensors clarify  
628 membrane receptor activation. *Nat Chem Biol* **13**, 372-380 (2017).
- 629 45. Pagano, A. et al. C-terminal interaction is essential for surface trafficking but not for  
630 heteromeric assembly of GABA<sub>B</sub> receptors. *J. Neurosci.* **21**, 1189–1202 (2001).
- 631 46. Isberg, V. et al. Generic GPCR residue numbers - aligning topology maps while  
632 minding the gaps. *Trends Pharmacol Sci* **36**, 22-31 (2015).
- 633 47. Calver, A.R. et al. The C-terminal domains of the GABA(b) receptor subunits mediate  
634 intracellular trafficking but are not required for receptor signaling. *J Neurosci* **21**,  
635 1203-1210 (2001).
- 636 48. Burmakina, S., Geng, Y., Chen, Y. & Fan, Q.R. Heterodimeric coiled-coil interactions  
637 of human GABAB receptor. *Proc Natl Acad Sci U S A* **111**, 6958-6963 (2014).
- 638 49. Guo, W. et al. Dopamine D2 receptors form higher order oligomers at physiological  
639 expression levels. *EMBO J* **27**, 2293-2304 (2008).
- 640 50. Villemure, J.F. et al. Subcellular distribution of GABA(B) receptor homo- and hetero-  
641 dimers. *Biochem J* **388**, 47-55 (2005).
- 642 51. Koehl, A. et al. Structural insights into the activation of metabotropic glutamate  
643 receptors. *Nature* **566**, 79-84 (2019).
- 644 52. Lecat-Guillet, N. et al. FRET-Based Sensors Unravel Activation and Allosteric  
645 Modulation of the GABAB Receptor. *Cell Chem Biol* **24**, 360-370 (2017).
- 646 53. Kaupmann, K. et al. GABA B-receptor subtypes assemble into functional heteromeric  
647 complexes. *Nature* **396**, 683-687 (1998).
- 648 54. Moller, T.C. et al. Oligomerization of a G protein-coupled receptor in neurons  
649 controlled by its structural dynamics. *Sci Rep* **8**, 10414 (2018).
- 650 55. Schwenk, J. et al. Native GABA(B) receptors are heteromultimers with a family of  
651 auxiliary subunits. *Nature* **465**, 231-235 (2010).
- 652 56. Venkatakrisnan, A.J. et al. Molecular signatures of G-protein-coupled receptors.  
653 *Nature* **494**, 185-194 (2013).
- 654 57. Weis, W.I. & Kobilka, B.K. The Molecular Basis of G Protein-Coupled Receptor  
655 Activation. *Annu Rev Biochem* **87**, 897-919 (2018).
- 656 58. Navarro, G. et al. Evidence for functional pre-coupled complexes of receptor  
657 heteromers and adenylyl cyclase. *Nat Commun* **9**, 1242 (2018).
- 658 59. Doumazane, E. et al. A new approach to analyze cell surface protein complexes  
659 reveals specific heterodimeric metabotropic glutamate receptors. *FASEB J* **25**, 66-77  
660 (2011).
- 661 60. Levitz, J. et al. Mechanism of Assembly and Cooperativity of Homomeric and  
662 Heteromeric Metabotropic Glutamate Receptors. *Neuron* **92**, 143-159 (2016).
- 663 61. Damian, M., Martin, A., Mesnier, D., Pin, J.P. & Baneres, J.L. Asymmetric  
664 conformational changes in a GPCR dimer controlled by G-proteins. *EMBO J* **25**,  
665 5693-5702 (2006).
- 666 62. Lancaster, E. et al. Antibodies to the GABA(B) receptor in limbic encephalitis with  
667 seizures: case series and characterisation of the antigen. *Lancet Neurol* **9**, 67-76  
668 (2010).
- 669 63. Doumazane, E. et al. Illuminating the activation mechanisms and allosteric properties  
670 of metabotropic glutamate receptors. *Proc Natl Acad Sci U S A* **110**, E1416-1425  
671 (2013).
- 672 64. Sali, A. & Blundell, T.L. Comparative protein modelling by satisfaction of spatial  
673 restraints. *J Mol Biol* **234**, 779-815 (1993).

- 674 65. Wu, H. et al. Structure of a class C GPCR metabotropic glutamate receptor 1 bound to  
675 an allosteric modulator. *Science* **344**, 58-64 (2014).
- 676 66. Larkin, M.A. et al. Clustal W and Clustal X version 2.0. *Bioinformatics* **23**, 2947-2948  
677 (2007).
- 678 67. Shen, M.Y. & Sali, A. Statistical potential for assessment and prediction of protein  
679 structures. *Protein Sci* **15**, 2507-2524 (2006).
- 680 68. Rasmussen, S.G. et al. Crystal structure of the beta2 adrenergic receptor-Gs protein  
681 complex. *Nature* **477**, 549-555 (2011).
- 682 69. Pettersen, E.F. et al. UCSF Chimera--a visualization system for exploratory research  
683 and analysis. *J Comput Chem* **25**, 1605-1612 (2004).
- 684 70. Waterhouse, A.M., Procter, J.B., Martin, D.M., Clamp, M. & Barton, G.J. Jalview  
685 Version 2--a multiple sequence alignment editor and analysis workbench.  
686 *Bioinformatics* **25**, 1189-1191 (2009).
- 687
- 688

689 **Acknowledgments**

690 We thank the Cisbio Bioassays for their support in providing reagents. J. L. was supported by  
691 the Ministry of Science and Technology (grant number 2018YFA0507003), the National  
692 Natural Science Foundation of China (NSFC) (grant numbers 81720108031, 81872945,  
693 31721002 and 31420103909), the Program for Introducing Talents of Discipline to the  
694 Universities of the Ministry of Education (grant number B08029), and the Mérieux Research  
695 Grants Program of the Institut Mérieux. P. R. and J.-P. P. were supported by the Centre  
696 National de la Recherche Scientifique (CNRS), the Institut National de la Santé et de la  
697 Recherche Médicale (INSERM), and by grants from the Agence Nationale de la Recherche  
698 (ANR-09-PIRI-0011), the FRM (Equipe FRM DEQ20130326522 and DEQ20170336747). L.  
699 X. was supported by a doctoral fellowship from the French Embassy in China and X. R. by a  
700 post-doctoral fellowship from the Agència de Gestió d'Ajuts Universitaris i de Recerca  
701 (AGAUR) and the Spanish Ministry of Economy, Industry and Competitiveness (SAF2015-  
702 74132-JIN).

703

704 **Author contributions**

705 L.X., Q.S., H.Z., X.R., S.G., Q.H., J.-P.P., J.L. and P.R. designed experiments; L.X., Q.S.,  
706 H.Z., S.G. and Q.H. performed molecular biology, cross-linking, functional assays; L.X.,  
707 Q.S., H.Z., X.R., J.-P.P., J.L. and P.R. performed data analysis; X.R. performed molecular  
708 modelling; L.X., J.L., J.-P.P. and P.R. wrote the manuscript.

709

710 **Competing interests**

711 The authors declare no competing interests.

712

713 **Figure legends**

714

715 **Figure 1**

716 **Schematic representation of the GABA<sub>B</sub> receptor**

717 **(a)** GABA<sub>B</sub> forms an obligatory heterodimer made of the two subunits GABA<sub>B1</sub> (GB1, blue)  
718 and GABA<sub>B2</sub> (GB2, grey). GABA binds to the extracellular domain (ECD) of GB1, while the  
719 GB2 heptahelical domain (7TM) is responsible for G-protein activation. **(b)** GABA<sub>B</sub> has the  
720 tendency to form stable higher-order hetero-oligomers that are likely organized through  
721 interactions between the GB1 subunits, while GB2 is likely not directly involved in these  
722 contacts. **(c)** Recently reported loss-of-function genetic mutations in GB2 7TM in human  
723 diseases. Most of these mutations affect residues in GB2<sup>TM6</sup> (Gly693, yellow; Ser695, red;  
724 Ile705, orange; Ala707, cyan). These mutations produce a constitutively active receptor,  
725 except the mutation of Gly693 that has not been studied in functional assays.

726

727 **Figure 2**

728 **Cysteine cross-linking identifies TM5 and TM6 at the 7TM heterodimer interface**

729 **(a)** Schematic representation of the GB1<sup>Ctr</sup> and GB2<sup>Ctr</sup> constructs used in the study. To easily  
730 distinguish GB1-GB2 and GB1-GB1 cross-linking in SDS-PAGE experiments, the molecular  
731 weight of the two subunits was modified. The SNAP-tagged full-length GB1 was truncated in  
732 the C-terminal region downstream of the coil-coiled region. Halo-tagged full-length GB2 was  
733 enlarged by adding a GFP tag at the C-terminal end of the subunit. To prevent the endogenous  
734 Cys producing unwanted disulfide bridges, the two indicated Cys residues in GB2<sup>TM4</sup> were  
735 changed to alanine. **(b)** 3D model of the 7TM of GB1 (blue) and GB2 (grey). All cysteine  
736 substitutions are highlighted by a yellow ball ( $\alpha$  carbon), and those that cross-linked well in  
737 TM5 and TM6 (see panel *c*) by a red ball. **(c)** Cross-linking of the indicated cell surface  
738 SNAP-GB1 subunits labeled with fluorescent SNAP substrates, after treatment (+) or without

739 treatment (-) with CuP. After SDS-PAGE in non-reducing conditions, GB1 monomers and  
740 GB1-GB2 dimers were detected via the fluorophore covalently attached to the receptors. MW,  
741 molecular weight. Data are representative of a typical experiment performed three times. **(d)**  
742 Change of GB1-GB2 dimer rate induced by CuP treatment for the “Control” heterodimer  
743 (GB1<sup>Ctrl</sup> co-expressed with GB2<sup>Ctrl</sup>) and every indicated mutant (both GB1 and GB2 subunits  
744 having a Cys residue in the same position). Positions with a significant change were  
745 highlighted in red. Data are mean  $\pm$  SD from at least three independent experiments (n = 3-6).  
746 Unpaired t test with Welch's correction with \*\*\*\* P<0.0001 and \*\*\* P<0.001, the other data  
747 being not significant. **(e)** Dimerization interface based on the results of the cross-linking  
748 experiments in the absence of ligand. TMs that can cross-link between GB1 and GB2 are  
749 highlighted in red.

750

### 751 **Figure 3**

#### 752 **The interface of the heterodimer is switched from TM5 to TM6 during activation**

753 **(a-b)** The cell surface SNAP-GB1 containing the indicated single cysteine substitution was  
754 cross-linked with the indicated GB2 cysteine mutant. The results were obtained for the  
755 symmetric interface TM5 and TM6, after pre-incubation with the agonist GABA or the  
756 competitive antagonist CGP54626 and with CuP. The percentage of GB1-GB2 heterodimers  
757 (in red) and GB1-GB1 homodimers (in blue) relative to the total amount of GB1 subunit was  
758 quantified by imaging the fluorescent blots. **(c)** Change of GB1-GB2 dimer rate induced by  
759 the agonist and determined by GB1-GB2 dimer quantification before and after GABA  
760 treatment. Data are mean  $\pm$  SD from at least three independent experiments (n = 3-5).  
761 Unpaired t test with Welch's correction with \*\*\*\* P<0.0001, \*\*\* P<0.001 and \*\* P<0.01, the  
762 other data being not significant. GABA and CGP54626 were used at 100  $\mu$ M. **(d)** Model  
763 highlighting the TMs involved in the dimerization of GB1-GB2 heterodimers in the inactive  
764 state (TM5, yellow) and in the active state (TM6, red).

765

766 **Figure 4**

767 **Disulfide cross-linking confirms the GB1-GB2 TM6 active interface and the resting**  
768 **interface**

769 **(a)** Inositol phosphate (IP) production in cells that co-express the mutants GB1<sup>6.59</sup> and GB2<sup>6.59</sup>  
770 after treatment with or without CuP, and stimulation with GABA. Results are mean ± SD  
771 from three independent experiments performed in triplicates. **(b)** In both the control receptor  
772 (after stimulation with GABA) and the co-expressed mutants GB1<sup>6.59</sup> and GB2<sup>6.59</sup>, IP  
773 production is proportional to the amount of SNAP-tagged GB1 at the cell surface, as  
774 measured by fluorescence after labeling with SNAP-Red substrate and then treatment with  
775 CuP. GABA was used at 100 μM. Data are mean ± SD from a typical experiment performed  
776 three times. **(c)** Treatment with the indicated competitive antagonist does not reverse the  
777 constitutive activity after GB1-GB2 TM6s cross-linking. GABA and CGP54626 were used at  
778 1 μM and 10 μM, respectively. Data are mean ± SEM from a typical experiment performed  
779 three times. Unpaired t test with Welch's correction with \* P<0.1, *ns*, not significant. **(d-f)**  
780 Stabilizing the inactive GB1-GB2 interface (*d*) by co-expressing the indicated mutants that  
781 cross-link well upon CuP treatment (*e*), impairs IP accumulation induced by GABA (*f*). Data  
782 are mean ± SD from a typical experiment performed three times.

783

784 **Figure 5**

785 **Rearrangement of the transmembrane domain interface during GABA<sub>B</sub> heterodimer**  
786 **activation**

787 3D model of the GB1-GB2 7TM heterodimer **(a)** and mGluR2 7TM homodimer **(b)** in the  
788 resting and active orientations. Based on these models, the amplitude of the relative

789 reorientation of two 7TMs in the dimer might be smaller in the GABA<sub>B</sub> receptor than in  
790 mGluR2.

791

792

793 **Figure 6**

794 **Interactions between GB1 7TMs in GABA<sub>B</sub> oligomers during activation**

795 **(a,b)** Schematic representation of a GABA<sub>B</sub> oligomer in lateral (*a*) and top view (*b*). **(c,d)**  
796 Blots showing cross-linking of cell surface SNAP-GB1 subunits containing a single cysteine  
797 substitution in TM1, TM4, TM5, TM6 or TM7, with GB2<sup>Ctr</sup> after pre-incubation or not with  
798 GABA (agonist) and with CuP, as indicated. The percentage of GB1-GB1 homodimers (in  
799 red) relative to the total amount of GB1 subunit was quantified from the fluorescent images.  
800 Data are mean ± SD from three independent experiments. Paired t test with Welch's correction  
801 with \*\*\*\* P<0.0001, \*\*\* P<0.001 and \*\* P<0.01, or not significant (ns). **(e,f)** Model for the  
802 structural organization of the GABA<sub>B</sub> 7TMs in higher-order oligomers in the inactive and  
803 active state. Interfaces at the GB1 subunits are highlighted.

804

805 **Figure 7**

806 **High-molecular-weight complexes confirm the two interfaces between GB1s in oligomers**

807 **(a)** Quantification of the oligomers obtained after cross-linking of the double cysteine  
808 substitution in different TMs of the GB1 subunit, after pre-incubation or not with GABA and  
809 with CuP, as indicated. The percentage of oligomers (in purple) relative to the total amount of  
810 GB1 subunit was quantified from the fluorescent blots. The pictograms indicate the possible  
811 cross-linking of three GB1 subunits that could form the oligomer band of the corresponding  
812 blot. These schemes are from snapshots of the GABA<sub>B</sub> oligomer 3D model when morphing  
813 are performed between the inactive and active states (see Fig. 9a and 9b). GABA was used at  
814 100 μM. Data are mean ± SD of at least three individual experiments (n = 3-5). Paired t test

815 with Welch's correction with \*\*\*  $P < 0.001$ , \*\*  $P < 0.01$  and \*  $P < 0.1$ , the other data being not  
816 significant (ns). **(b)** Quantification of the oligomers (% of total GB1) obtained for the  
817 indicated pairs of cysteines in *panel a*, after cross-linking in presence of CuP and GABA. **(c)**  
818 Model of the 7TM of GABA<sub>B</sub> oligomers highlighting the two distinct and possible interfaces  
819 between the GB1 subunits during activation.

820

## 821 **Figure 8**

### 822 **A disease-causing mutation stabilizes the active interface of the dimer and oligomer**

823 **(a,b)** Quantification of the GB1-GB2 cross-linking for the GB1<sup>6.56</sup> and GB2<sup>6.56</sup> cysteine  
824 mutants containing or not the genetic mutation S695I<sup>6.42</sup> in the GB2 subunit, in the indicated  
825 conditions and as described in *Fig. 3*. Both cysteine mutation and the genetic mutation have  
826 been introduced in the rat GB1<sup>Ctr</sup> and GB2<sup>Ctr</sup>. **(c,d)** Quantification of the GB1-GB1 cross-  
827 linking for the GB1<sup>5.42</sup> single cysteine mutant co-expressed with GB2<sup>Ctr</sup> containing or not the  
828 genetic mutation S695I<sup>6.42</sup>. GABA and CGP54626 were used at 100  $\mu$ M. Data are mean  $\pm$  SD  
829 from at least three independent experiments ( $n = 3-5$ ). Unpaired t test with Welch's correction  
830 with \*\*\*\*  $P < 0.0001$ , or not significant (ns).

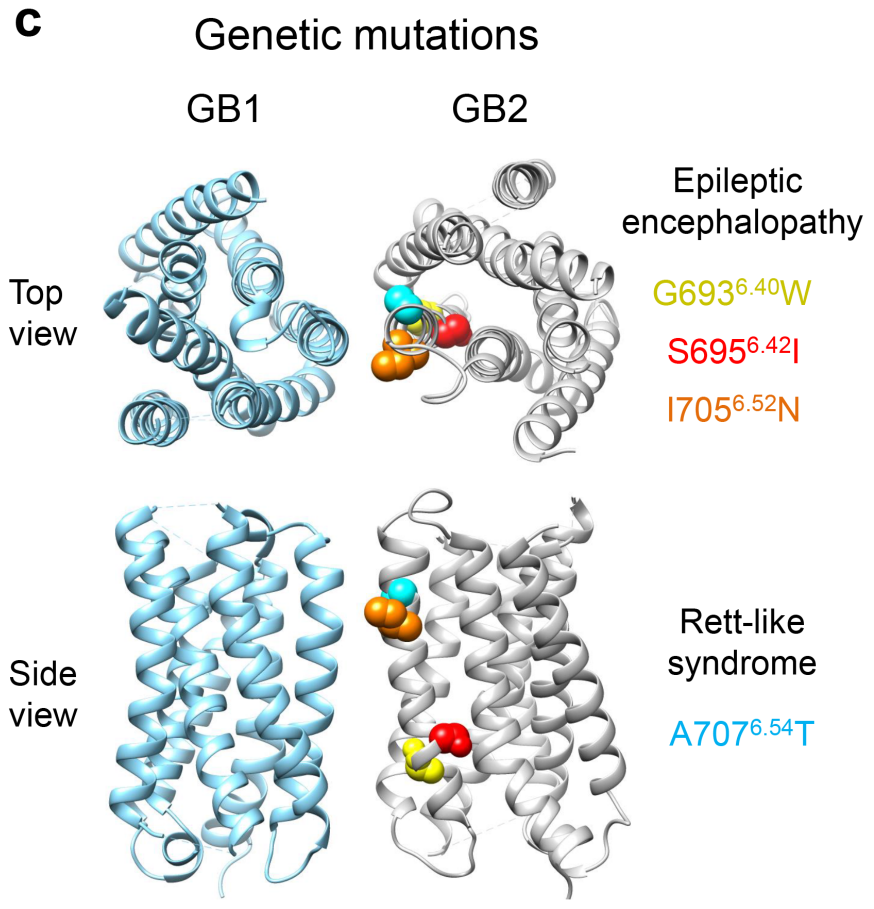
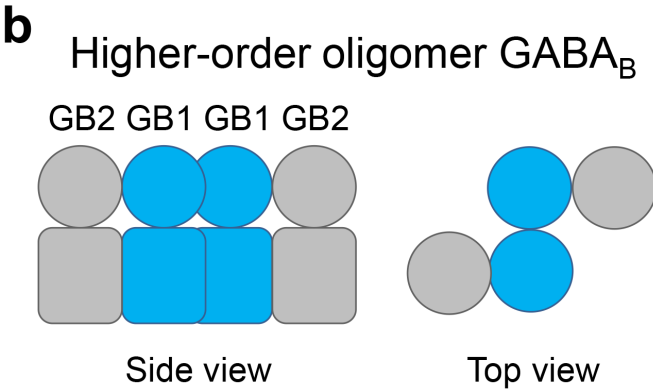
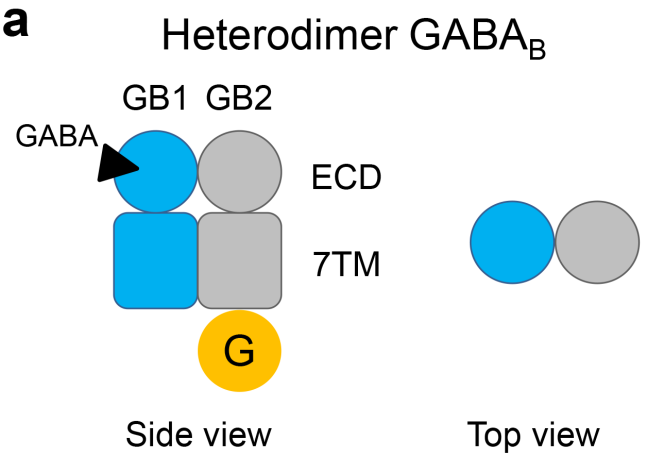
831

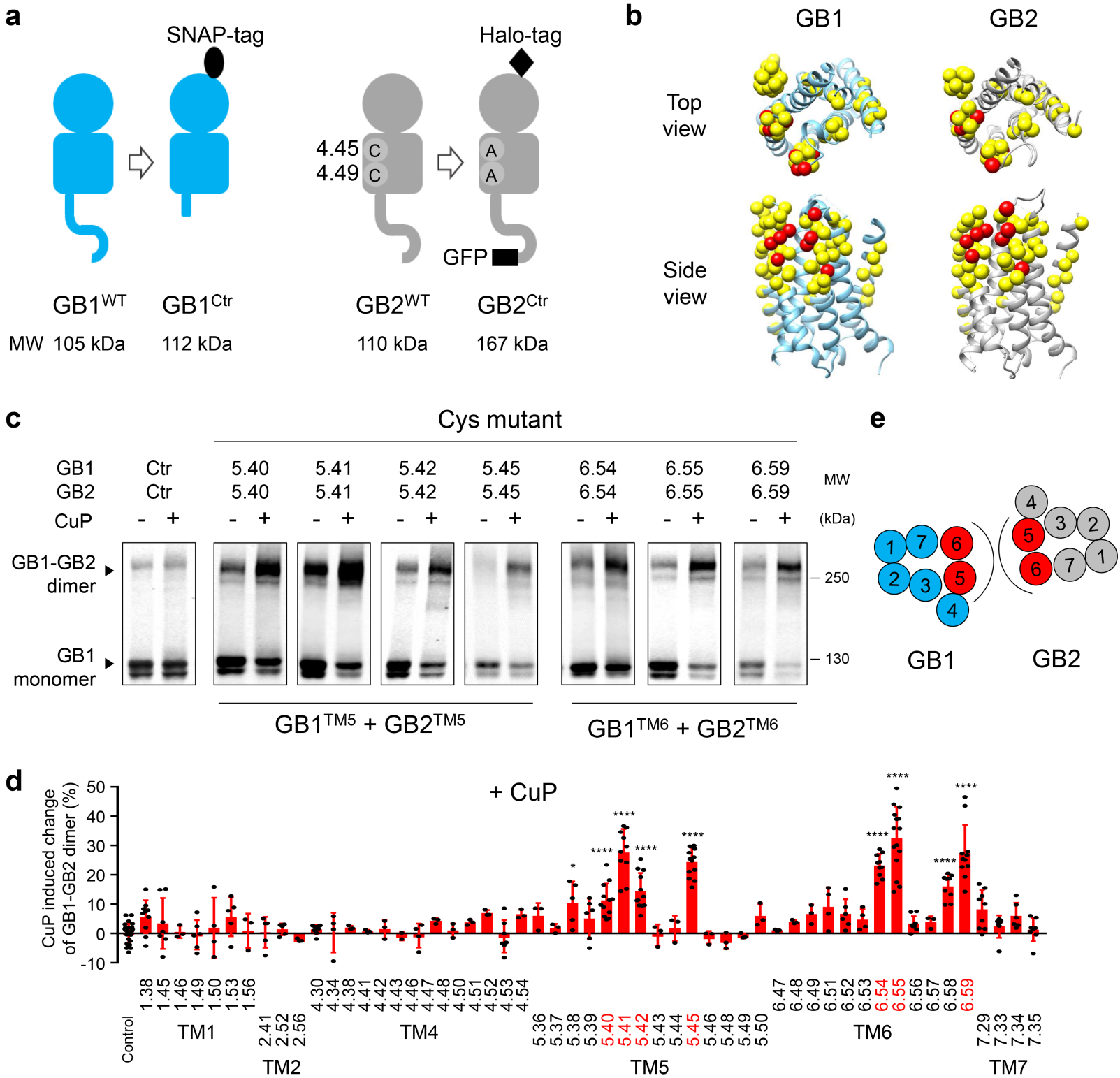
## 832 **Figure 9**

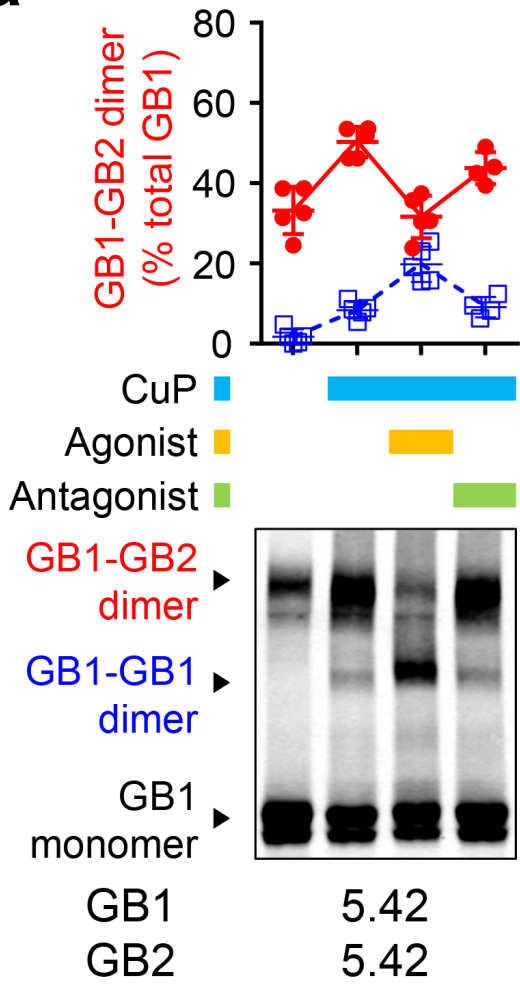
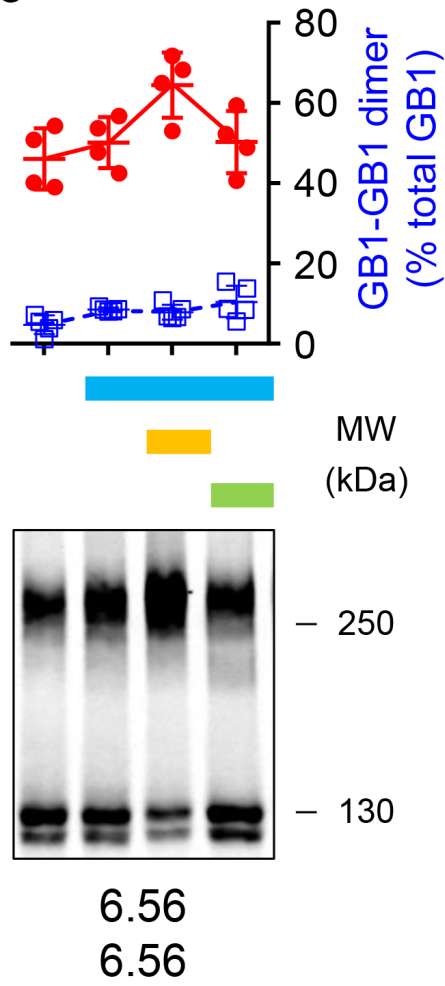
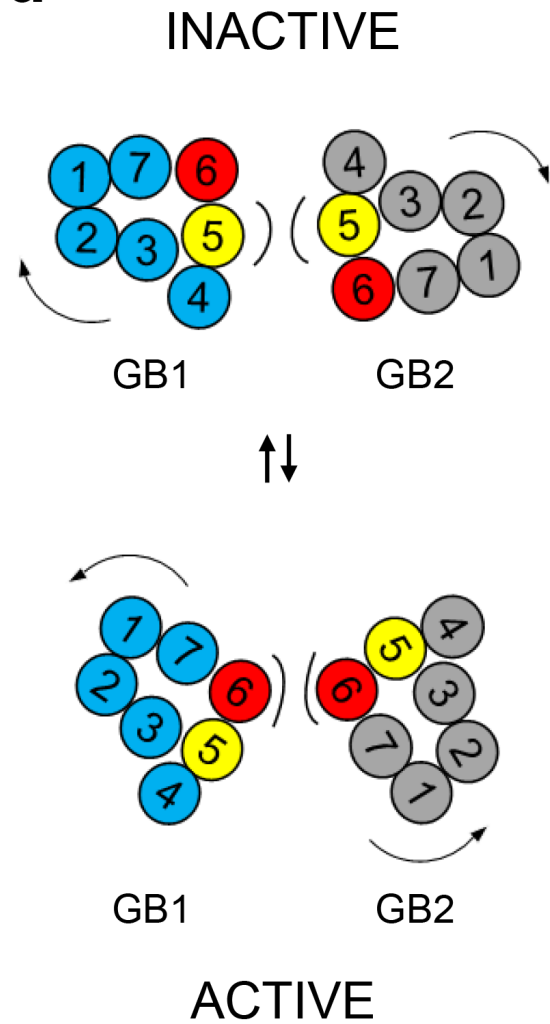
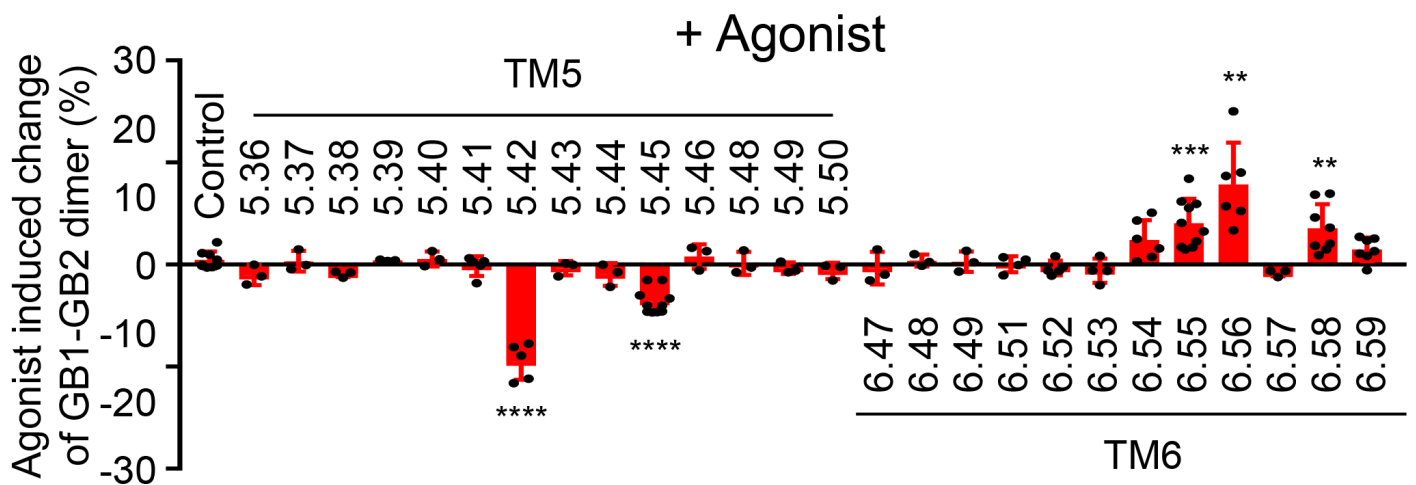
### 833 **Agonist-induced rearrangement of the 7TMs in the GABA<sub>B</sub> oligomer during activation**

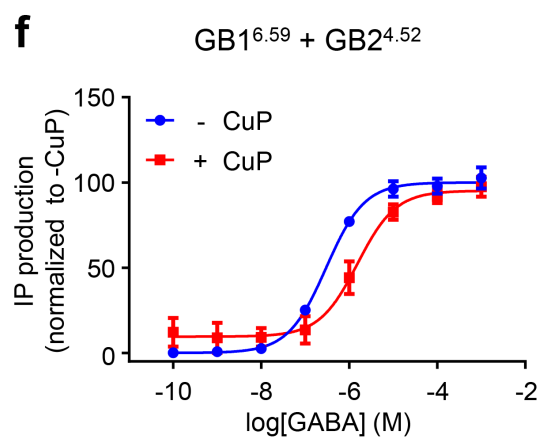
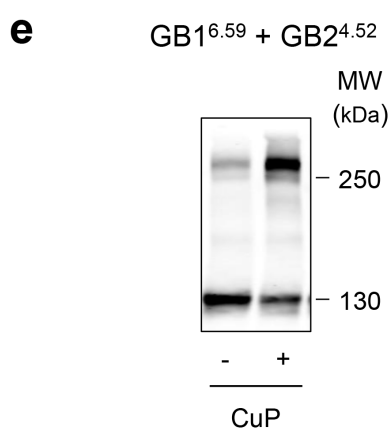
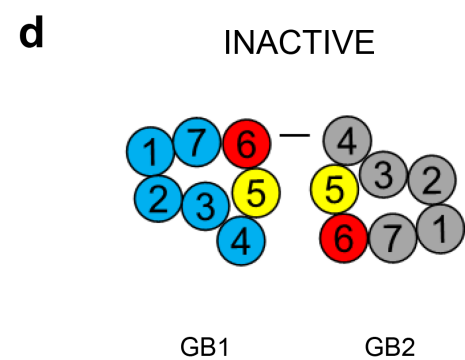
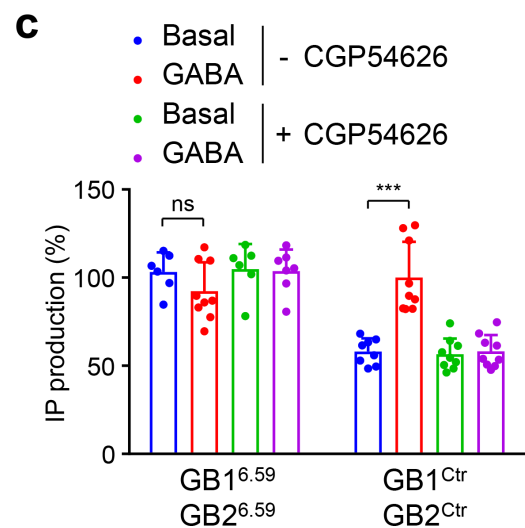
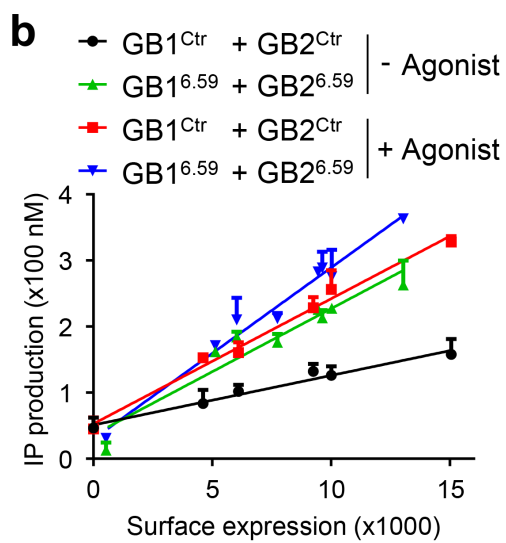
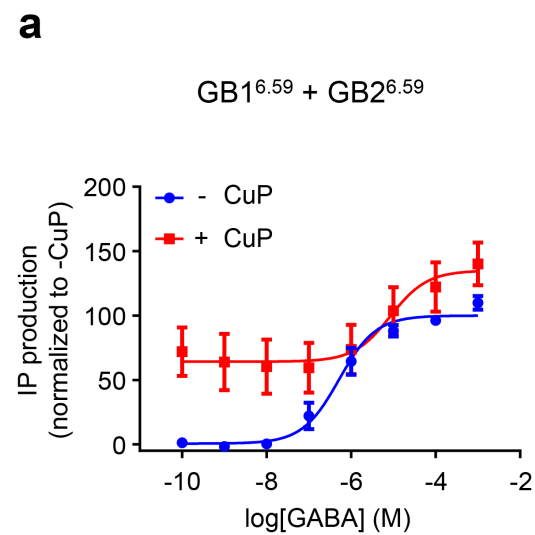
834 **(a,b)** 3D model of the 7TM oligomer in the inactive and active orientations. The dashed line  
835 highlights a minimal functional receptor made of GB1 and GB2 (heterodimer *B*). Heterodimer  
836 *A* is proposed to assemble the tetramer with *B*, and *C* to form oligomer with the tetramer *A-B*.  
837 In this model, stabilization of the tetramer interactions is made by the symmetric interfaces  
838 with GB1<sup>TM6</sup> in the resting state, and with GB1<sup>TM1-TM7</sup> in the active state. Stabilization of the  
839 oligomer would be through the symmetric interfaces with GB1<sup>TM4</sup> in the resting state and with

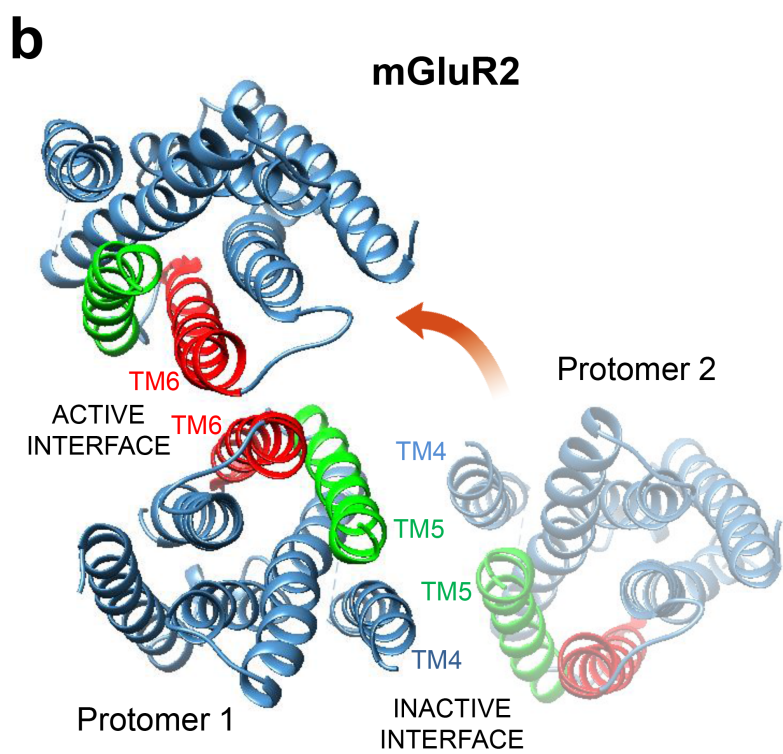
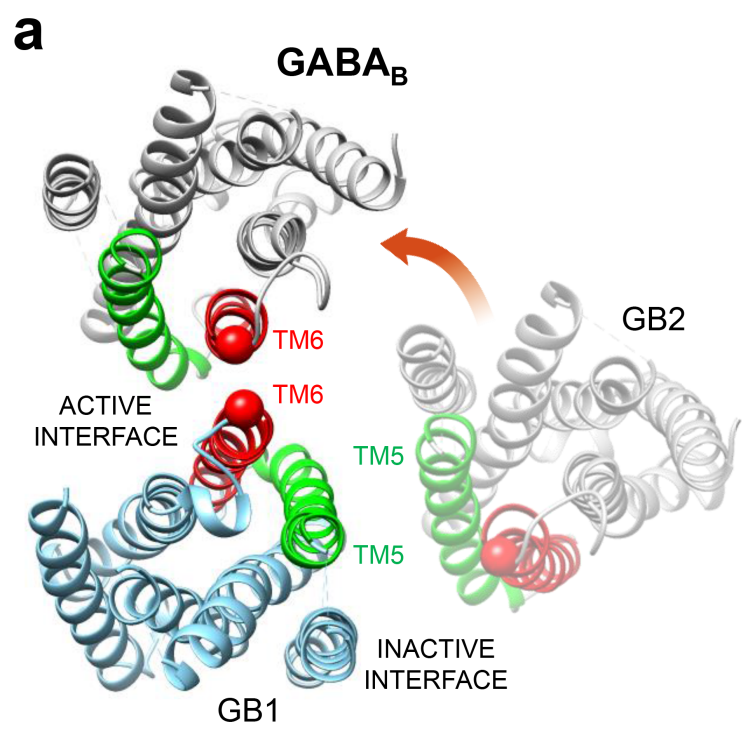
840 GB1<sup>TM4-TM5</sup> in the active state. TM4, TM5 and TM6 of GB1 and GB2 are in yellow, green  
841 and red, respectively. (c) Model of the active oligomer coupled to four G $\alpha\beta\gamma$  proteins based  
842 on the structure of the complex between the active  $\beta_2$ -adrenergic receptor and the G protein  
843 previously reported<sup>68</sup>.  
844





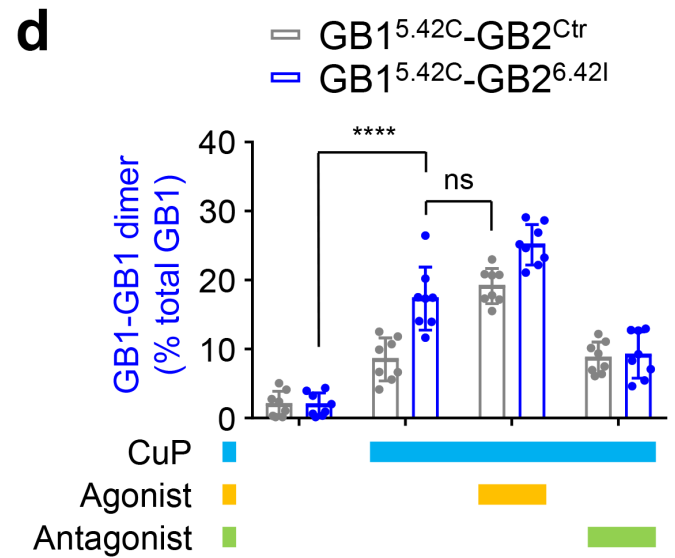
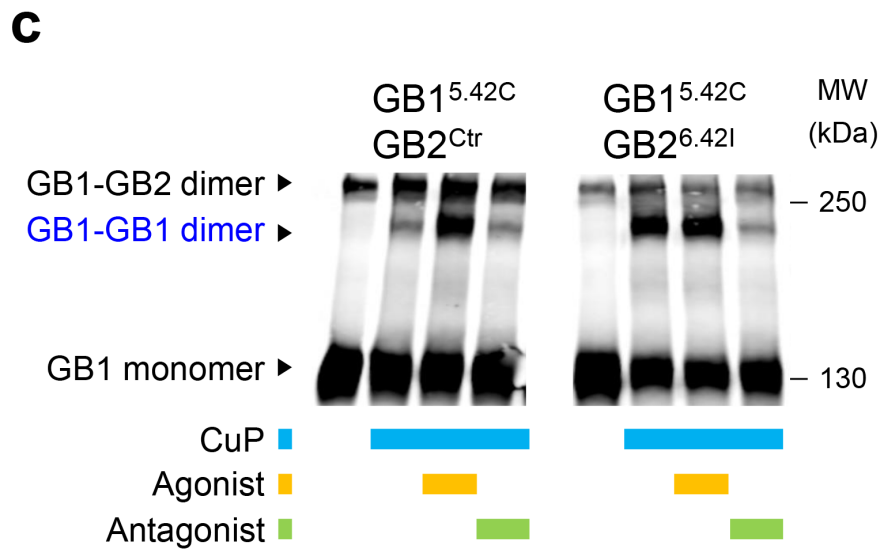
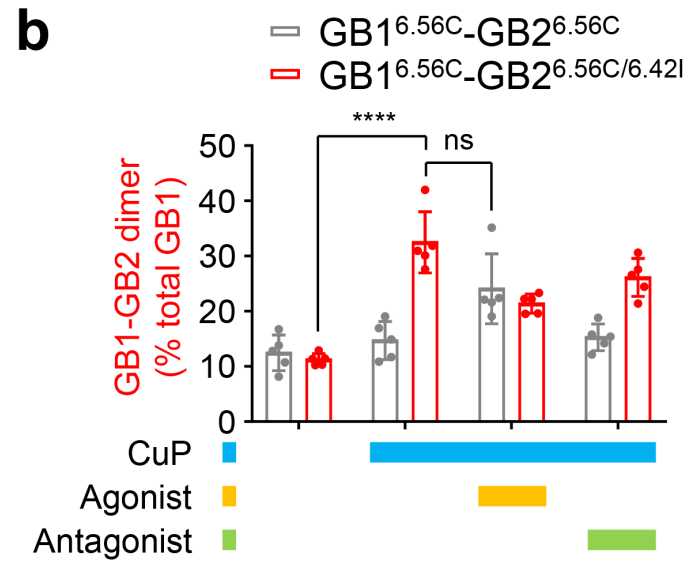
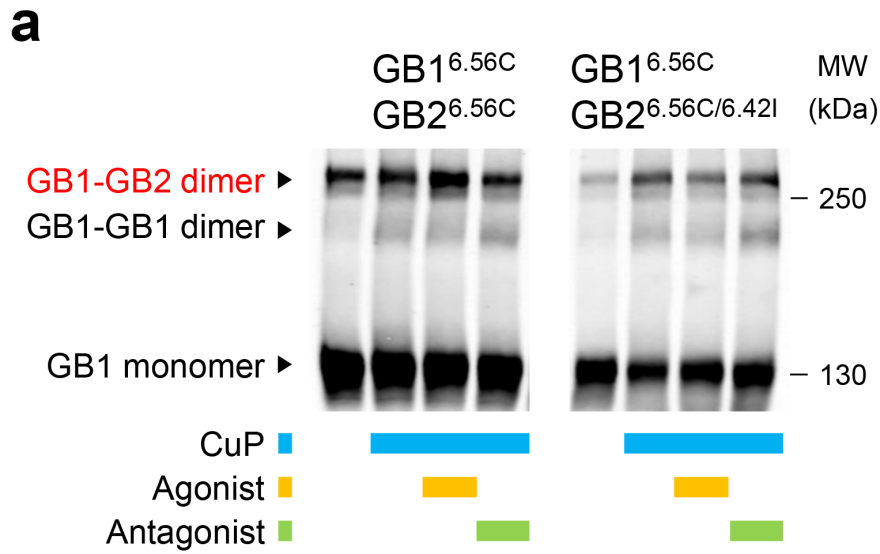
**a****b****d****c**



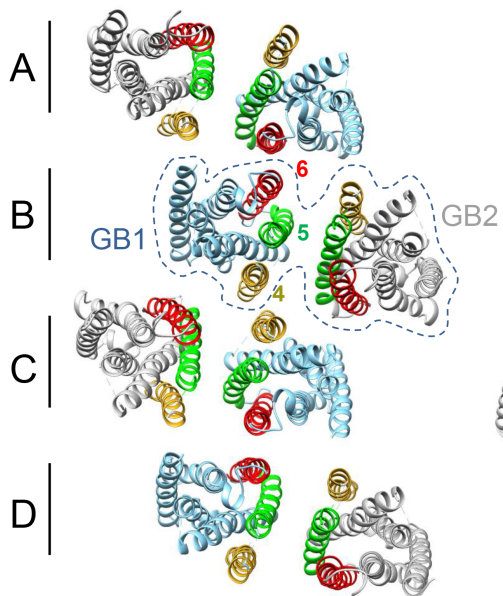




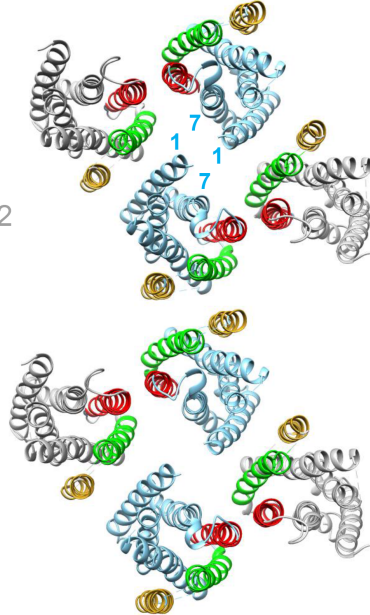




**a Inactive**



**b Active**



**c Active + G protein**

